RESEARCH ARTICLE

The FASEB Journal

AP2XII-9 is essential for parasite growth and suppresses bradyzoite differentiation in *Toxoplasma gondii*

Xiao-Jing Wu[1,2] | Meng Wang[1] | Nian-Zhang Zhang[1] | Ting-Ting Li[1] |
Jin Gao[1,2] | Li-Xiu Sun[1] | Xing-Quan Zhu[2] | Jin-Lei Wang[1]

[1]State Key Laboratory for Animal Disease Control and Prevention, Key Laboratory of Veterinary Parasitology of Gansu Province, Lanzhou Veterinary Research Institute, Chinese Academy of Agricultural Sciences, Lanzhou, People's Republic of China

[2]Laboratory of Parasitic Diseases, College of Veterinary Medicine, Shanxi Agricultural University, Taigu, People's Republic of China

Correspondence
Xing-Quan Zhu, Laboratory of Parasitic Diseases, College of Veterinary Medicine, Shanxi Agricultural University, Taigu, Shanxi Province 030801, People's Republic of China.
Email: xingquanzhu1@hotmail.com

Jin-Lei Wang, State Key Laboratory for Animal Disease Control and Prevention, Key Laboratory of Veterinary Parasitology of Gansu Province, Lanzhou Veterinary Research Institute, Chinese Academy of Agricultural Sciences, Lanzhou, Gansu Province 730046, People's Republic of China.
Email: wangjinlei90@126.com

Abstract

Cyst formation, resulting from the differentiation of rapidly replicating tachyzoites into slowly growing bradyzoites, is the primary cause of chronic toxoplasmosis. Although the mechanisms governing bradyzoite differentiation have been partially elucidated, they remain incompletely understood. In this study, we show that the transcription factor AP2XII-9 is localized in the nucleus and exhibits periodic expression during the tachyzoite stage, with peak expression observed during the synthesis and mitosis phases. Conditional knockdown of AP2XII-9 in both the type I RH strain and type II cyst-forming Pru strain revealed that AP2XII-9 plays a critical role in the lytic cycle by regulating the formation of the inner membrane complex, proper apicoplast inheritance, and normal cell division, underscoring its essential role in *T. gondii* growth. Furthermore, depletion of AP2XII-9 induced bradyzoite differentiation even in the absence of alkaline stress. Transcriptomic analysis revealed that the deletion of AP2XII-9 resulted in the downregulation of tachyzoite growth-related genes and upregulation of a series of bradyzoite-specific genes. Taken together, these findings indicate that AP2XII-9 is essential for maintaining the rapid and normal replication of tachyzoites while actively repressing bradyzoite differentiation, reflecting the complexity of the mechanisms underlying bradyzoite differentiation.

KEYWORDS

AP2XII-9, apicoplast inheritance, asynchronous division, bradyzoite differentiation, growth, membrane defect, *Toxoplasma gondii*

1 | INTRODUCTION

Toxoplasma gondii, the causative agent of toxoplasmosis, is a zoonotic parasitic protozoan known for infecting a broad range of hosts and its ability to flexibly switch between different developmental stages.[1–3] This parasite has infected approximately one-third of the global population, a testament to its highly effective infection strategy.[4,5] The balance between its replication and persistence is modulated by the host immune system and *T. gondii's* multiple developmental cycles. This balance is exemplified by the differentiation of rapidly replicating tachyzoites into slowly growing bradyzoites under immune pressure, leading to chronic infection. Conversely, immunosuppression enables rapid tachyzoite proliferation or reactivation of bradyzoites, which may result in severe or fatal outcomes for the host.[5,6] Currently, no effective drugs or vaccines are available to target the chronic stages of toxoplasmosis.

To establish acute infection, *T. gondii* must continuously complete the lytic cycle, beginning with replication after invading host cells. However, its replication pattern differs from that of other eukaryotic cells. The cell cycle of *T. gondii* consists of the gap 1 phase (G1), synthesis phase (S phase), mitosis phase (M phase), and cytokinesis phase (C phase), with either a very short or absent gap 2 phase (G2 phase).[7] *T. gondii* tachyzoite replication is characterized by endodyogeny, a unique form of binary fission where two daughter cells are assembled within the mother cell. This process involves a highly coordinated sequence of events, including DNA replication, mitosis, and the assembly of daughter cells within the cytoplasm of the mother.[8–11] Daughter cells begin budding during the late S phase, with organelles and other cellular components segregated and packaged into the developing daughters.[8,9] Once the budding process is complete, the mother cell disassembles, and the daughter cells emerge, acquiring their plasma membrane from the mother.[8,10] The entire process is tightly regulated by both transcriptional regulation and posttranslational modification (PTM), ensuring proper coordination between organelle biogenesis, cytoskeletal organization, and cytokinesis.[12–14] This replication strategy ensures internal stability within *T. gondii*, establishing a reliable mechanism for efficient infection and parasite propagation.

When the host immune system is robust, *T. gondii* tachyzoites undergo a developmental switch to the slowly replicating bradyzoite stage, forming tissue cysts that contribute to chronic infection. This differentiation is accompanied by significant changes in gene expression, protein synthesis, and energy metabolism that are tightly regulated by a complex network including transcription factors and PTM.[15–17] For example, the transcription factor BFD1, a master regulator of bradyzoite differentiation, binds to the promoter region of BFD2, co-regulating the bradyzoite differentiation process in a positive regulatory hierarchy.[15,16] Additionally, PP2A, a protein phosphatase, regulates bradyzoite differentiation, potentially by dephosphorylating key transcription factors involved in this developmental process, as indicated by the increased phosphorylation levels of BFD2 upon PP2A deletion.[17] However, the intricate regulatory network involving BFD1, BFD2, and PP2A remains poorly understood and requires further investigation.[17]

Several transcription factors have been demonstrated to regulate gene expression and play crucial roles in the development of various species.[15–23] The Apetala-2 (AP2) family, a transcription factor family first characterized in plants, is involved in important physiological and biological processes, including morphogenesis, stress response, and metabolic regulation.[23] Recently, members of the AP2 family have been identified as key transcriptional regulators involved in the replication and stage differentiation of *T. gondii*.[18–22] Some AP2 factors display distinct expression patterns, including periodic expression and stage expression, suggesting that precise gene regulation is essential for coordinating parasite infection and stage differentiation.[24–28] Studies have shown that AP2 factors can act as either activators or repressors, modulating the timed progression of bradyzoite differentiation. For example, AP2IV-4, AP2IX-4, AP2XII-2, and AP2IX-9 inhibit bradyzoite formation, while AP2XI-4 and AP2IV-3 function in the opposite manner.[19,20,24–27]

Given the pivotal roles of AP2 transcription factors in *T. gondii* and other apicomplexan parasites, the specific functions of several members of the AP2 family remain unclear. AP2XII-9, a factor predicted to have periodic expression peaking in the S/M phase, was selected for further investigation in this study to broaden our understanding of the biological functions of AP2 factors in *T. gondii*. Conditional knockout strains of AP2XII-9 were generated using the mini auxin-inducible degron (mAID) system combined with CRISPR-Cas9 technology. Depletion of AP2XII-9 resulted in significant growth defects, impairing invasion, intracellular replication, and egress processes, and was associated with abnormal morphology and structural defects. Additionally, the inactivation of AP2XII-9 induced tachyzoites to bradyzoites conversion, evidenced by the upregulation of bradyzoite-specific genes, as shown through bradyzoite conversion assays and RNA sequencing analysis. These findings demonstrate that AP2XII-9 plays critical roles in *T. gondii* growth, maintaining membrane and apicoplast integrity, and regulating cyst formation.

2 | MATERIALS AND METHODS

2.1 | Cell and parasite culture

All tachyzoites used in this study, including RHΔ *ku80*Δ*hxgprt*::TIR1 (referred as RH::TIR1), PruΔ*ku80* Δ*hxgprt*::TIR1 (referred as Pru::TIR1),[18] RHΔ*ku80*Δ *hxgprt*::TIR1-AP2XII-9-mAID-6HA (RH::TIR1-AP2XII-9-mAID), and PruΔ*ku80*Δ*hxgprt*::TIR1-AP2XII-9-mAID-6HA (Pru::TIR1-AP2XII-9-mAID), were cultured in monolayers of human foreskin fibroblasts (HFFs, ATCC SCRC-1041TM) in DMEM (Thermo Fisher Scientific, MA, USA) supplied with 1% heat-inactivated fetal bovine serum (FBS) (Thermo Fisher Scientific, MA, USA), 10 mM HEPES (pH 7.2, Solarbio, China), 100 U/mL of penicillin, and 100 μg/mL of streptomycin (Solarbio, China) at 37°C and 5% CO_2, as described previously.[17,18,29] The tachyzoites harvested from heavily infected HFF monolayers, released using a 27-gauge needle (BD Medical, USA), were used for subsequent experiments.

2.2 | Construction of the C-terminal conditional knockout strains of AP2XII-9

The mini auxin-inducible degron (mAID) system combined with CRISPR-Cas9 technology was used to construct conditional knockout strains of AP2XII-9 as previously described.[17,18,30] Briefly, the CRISPR-Cas9 plasmid targeting the 3′ UTR after the stop codon of AP2XII-9 and the corresponding degraded fragment including mAID-6HA and a DHFR marker were electroporated into the RH::TIR1 and Pru::TIR1 strains. After 3 μM pyrimethamine selection and gradient dilution, positive clones were identified by PCR, DNA sequencing, and immunofluorescence assay (IFA). Depletion of AP2XII-9 was achieved by treating the AP2XII-9-mAID strains with 500 μM 3-indoleacetic acid (IAA). All plasmids and primers used in the study are listed in supplementary material (Table S1).

2.3 | Antibodies

Primary antibodies include rabbit anti-IMC1, rabbit anti-ISP1, rabbit anti-CPN60, rabbit anti-GAP45, rabbit anti-β-tubulin (Tub), rabbit anti-MIC2, rabbit anti-ARO, rabbit anti-SERCA, rabbit anti-HSP60, mouse anti-IMC1, mouse anti-GRA5, rabbit anti-BAG1, rabbit anti-aldolase (ALD) (1:500, available in our laboratory and validated in our published paper),[17,18,31–33] mouse anti-HA (1:500, purchased from BioLegend, San Diego, USA), rabbit anti-HA, mouse anti-SAG1 (1:1000, Invitrogen, USA). The secondary antibodies include Alexa Fluor 488 goat anti-rabbit IgG (H + L), Alexa Fluor 488 goat anti-mouse IgG (H + L), Alexa Fluor 594 goat anti-rabbit IgG, Alexa Fluor 594 goat anti-mouse IgG, Alexa Fluor 647 goat anti-rabbit IgG (1:500, Invitrogen, USA), goat anti-rabbit HRP (1:1000, biodragon, China), and FITC-*Dolichos Biflorus* lectin (DBL, Vector Laboratories) (1:500). 4′, 6-diamidino2-phenylindole (DAPI) was used to stain parasites and host nuclei. Treated samples were imaged with a Leica confocal microscope system (TCS SP8, Leica, Germany).

2.4 | Indirect immunofluorescence analysis

Tachyzoites infected HFFs were fixed with 4% paraformaldehyde (PFA) for 30 min, permeabilized with 0.1% Triton X-100 for 20 min at room temperature, and blocked with 5% bovine serum albumin (BSA) diluted in phosphate-buffered saline (PBS) for 2 h at 37°C. The samples were incubated with primary antibody for 2 h and secondary antibody for 1 h at 37°C, followed by DAPI for 10 min. Each incubation of samples, including fixation, permeabilization, blocking, and staining, required five washes with PBS. Images of the samples were obtained using a Leica confocal microscope system.

2.5 | Western blotting

Harvested parasites were lysed on ice for 1 h in RIPA buffer containing EDTA and protease inhibitor cocktail (Thermo Fisher Scientific, MA, USA). The lysate was centrifuged at 4°C for 10 min to collect the supernatant. Bands were separated by 10% SDS-PAGE gels and transferred to polyvinylidene fluoride (PVDF) membranes. The PVDF membranes were blocked with 5% skim milk for 2 h and incubated with primary antibodies (rabbit anti-ALD, rabbit anti-HA) and secondary antibodies (goat anti-rabbit HRP) for 2 h and 1 h at 37°C, respectively. Proteins were detected using the ECL chemiluminescent reagent (Thermo Fisher Scientific, MA, USA) and imaged using the Minichemi 610 chemiluminescent imager (Bio-Rad Laboratories, CA, USA).

2.6 | Plaque assay

Plaque assay was performed to evaluate the effect of AP2XII-9 on the growth ability of *T. gondii* as described previously.[31] Briefly, ~500 syringe-released AP2XII-9-mAID tachyzoites were infected with confluent HFFs in 12-well plates for 7 or 8 days in the presence or absence of

IAA. The samples were fixed with 4% PFA for 30 min and 0.5% crystal violet for 20 min at room temperature. The number and size of plaques were imaged by scanner and analyzed by ImageJ.[34] The plaque assays were performed in biological triplicate.

2.7 | Invasion assay

For invasion assay, ~10^6 tachyzoites were pretreated with or without IAA for 24 h before invasion. Then, tachyzoites were added to HFFs grown in 12-well plates and cultured for 30 min with or without IAA. After washing unbound tachyzoites with PBS, samples were fixed with 4% PFA for 30 min. IFA assay was performed to label external tachyzoites with mouse anti-SAG1 and Alexa Fluor 488 goat anti-mouse IgG. Samples were permeabilized with 0.1% Triton X-100 and stained all tachyzoites using rabbit anti-GAP45 and Alexa Fluor 594 goat anti-rabbit IgG. Three independent experiments were performed to determine the ratio of intracellular tachyzoites to total tachyzoites by counting at least 100 fields in each biological duplicate.

2.8 | Replication assay

Approximately 10^6 tachyzoites were added to HFFs to invade for 1 h, and uninvaded tachyzoites were washed away with warm DMEM. After incubation (24 h for RH::TIR1-AP2XII-9-mAID and 28 h for Pru::TIR1-AP2XII-9-mAID) with or without IAA, samples were fixed with 4% PFA for 30 min and permeabilized with 0.1% Triton X-100 for 20 min. Next, samples were incubated with primary antibody (rabbit anti-IMC1) and secondary antibody (Alexa Fluor 594 goat anti-rabbit IgG). Replication efficiency was determined by quantifying the number of tachyzoites within at least 100 parasitophorous vacuoles (PVs). The replication assay was repeated three independent times.

2.9 | Egress assay

Approximately 2×10^6 freshly egressed tachyzoites were allowed to invade confluent HFFs for 60 h or 36 h in the presence or absence of IAA. Once the number of PVs was basically consistent, samples were treated with 3 μM calcium ionophore A23187 (Sigma, Darmstadt, Germany) diluted with warm DMEM, and egress efficiency was evaluated with reference to at least 100 PVs as previously described.[31] The assay was performed in biological triplicate.

2.10 | In vitro tissue cyst differentiation assay

Tachyzoites to bradyzoites conversion in vitro was evaluated as previously described.[35] Briefly, approximately 2×10^5 tachyzoites were infected with HFFs grown in 12-well plates under normal culture conditions with or without IAA for 60 h. Parasites were labeled by mouse anti-IMC1 combined with Alexa Fluor 594 goat anti-mouse IgG, and bradyzoite cysts were detected by rabbit anti-BAG1 combined with Alexa Fluor 647 goat anti-rabbit IgG and FITC-DBL. At least 100 PVs were used to quantify cyst formation. The experiment was repeated three independent times.

2.11 | RNA sequencing

The Pru::TIR1-AP2XII-9-mAID strain, cultured for 72 h under normal culture conditions with or without IAA, was harvested for RNA sequencing. After scraping and releasing tachyzoites from HFFs, parasite pellets were harvested by centrifugation at 2000 rpm for 10 min and total RNA was extracted using the Trizol method. The quality and quantity of total RNA were examined using Nano Drop and Agilent 2100 bioanalyzer (Thermo Fisher Scientific, MA, USA). Libraries were established and sequenced using the BGI-AEQ platform (Shenzhen, China). High-quality reads were obtained by removing reads containing sequencing adapters, low-quality reads, and reads of unknown base ≥5% using SOAPnuke.[18] The filtered reads were aligned with the *T. gondii* ME49 reference genome (https://toxodb.org) using Bowtie2, and relative gene expression was calculated by the fragments per kilobase of per million mapped reads (FPKM) using RSEM.[36–38] Differential expression analysis was performed with DESeq2,[39] and Log$_2$ Fold Change ≥1 or ≤−1 and *Q*-value <0.05 were set as threshold for differentially expressed genes (DEGs).

2.12 | Real-time quantitative PCR (RT-qPCR)

RT-qPCR was performed as previously described.[35] The expression of eight randomly selected genes (five up-regulated and three down-regulated genes) of RNA samples was measured by the CFX96 Touch Real-Time PCR Detection System (Bio-Rad Laboratories, CA, USA) with β-tubulin as an internal reference. The reliability of gene expression obtained by RNA sequencing was verified by RT-qPCR. Each group of samples was analyzed

independently three times. All primers used in RT-qPCR are listed in supplementary material (Table S1).

2.13 | Bioinformatics analysis

The information on AP2XII-9, including the periodic expression profile, gene structure, and amino acid sequence, was retrieved from ToxoDB (https://toxodb.org/).[38] Domain prediction of AP2XII-9 was performed using the ExPASy Server (https://prosite.expasy.org/).[40] Based on the amino acid sequence of the AP2XII-9 protein, homologous proteins were screened by BLAST search equipped with VEuPathDB (https://veupathdb.org/) and the phylogenetic tree was constructed by the maximum likelihood method with a JTT matrix-based model in MEGA X software.[41–43]

2.14 | Statistical analysis

GraphPad Prism software version 8.0.1 was used for the statistical analysis. The analyzed data were obtained from at least three independent replicates. These results were presented as mean ± standard deviations (S.D.) and a p value < .05 was considered to be significant. All data and associated error bars, and significance analysis in this study can be found in the relevant figure legends.

3 | RESULTS

3.1 | AP2XII-9 is dynamically expressed in the nucleus and peaks in the S/M stage

A total of 68 AP2 factors have been identified in *T. gondii*, of which 12 AP2 factors have similar expression profiles that peak in the S/M stage of tachyzoites.[20] In this cohort, AP2IV-4, AP2IX-4, and AP2XII-2 act as transcriptional repressors, while AP2XI-4 acts as transcriptional activators in stage differentiation.[20,25,26,44] AP2XII-9 (TGME49_251740), the gene with the most negative parasite fitness value (−4.32) based on a genome-wide CRISPR-Cas9 screen,[20] was selected to further broaden the function of the AP2 family. AP2XII-9 protein contains 1893 amino acids with an AP2 domain (amino acids 403–455) at the N terminus and is encoded by two exons and one intron (Figure 1A). Phylogenetic analysis showed that AP2XII-9 was widely conserved across apicomplexan parasites including *Hammondia hammondi*, *Neospora caninum*, *Besnoitia besnoiti*, *Cystoisospora suis*, and *Plasmodium falciparum* (Figure 1B).

Considering the extremely negative phenotype value of AP2XII-9, a mAID system combined with CRISPR-Cas9 technology was employed to investigate the biological function of AP2XII-9 (Figure 1C). The mAID system uses 3-indoleacetic acid (IAA) to conditionally regulate the expression of AP2XII-9 on the basis of transport inhibitor response 1 (TIR1) and AP2XII-9 tagged with a mAID-6HA.[30] The successful construction of AP2XII-9-mAID strains was verified by PCR and IFA (Figure S1A, Figure 1D). The IFA assay showed that AP2XII-9 was expressed periodically in the nucleus and peaked at the S/M phase as predicted by the mRNA profile (Figure 1D, Figure S1B). To determine the precise timing of the expression of AP2XII-9, IMC sub-compartment proteins 1 (ISP1) and cytoskeleton markers β-tubulin were co-stained with AP2XII-9.[45,46] The co-staining of AP2XII-9 with ISP1 and β-tubulin confirmed that the expression of AP2XII-9 began before the formation of ISP1 daughter buds or the separation of centriole, gradually accumulated during the development of daughter buds, and became low or undetectable at the end of division (Figure S2A,B), confirming that AP2XII-9 is a cell cycle-expressed protein. In addition, effective degradation of AP2XII-9 was observed, as treatment of AP2XII-9-mAID strains with IAA for 24 h led to undetectable levels of the AP2XII-9 protein (Figure 1D).

3.2 | AP2XII-9 is critical for the growth of type I strain of *T. gondii*

Plaque assay was performed to investigate whether AP2XII-9 is involved in the growth of *T. gondii* type I strain. We found that there was no significant difference in plaque formation between the parental strain in the presence or absence of IAA and the AP2XII-9-mAID strain in the absence of IAA (Figure 2A–C). By contrast, the area and number of plaques formed by the AP2XII-9-mAID strain in the presence of IAA were significantly decreased (Figure 2A–C), indicating that AP2XII-9 plays essential roles in the growth of *T. gondii*.

The life activities of *T. gondii* are gradually proceeding through important lytic processes involved in cell invasion, replication, and egress.[47] Thus, invasion, intracellular replication, and egress assays were performed to further explore which steps of *T. gondii* growth were affected by the deletion of AP2XII-9 in the type I strain. For the invasion assay, AP2XII-9-mAID tachyzoites pretreated with or without IAA for 24 h were allowed to invade HFFs for 30 min. The invasion results showed a significant reduction in the invasion ability of the AP2XII-9-mAID strain in the presence of IAA (Figure 2D). Then, for the intracellular replication assay, AP2XII-9-mAID tachyzoites were allowed to invade without IAA for 1 h and cultured
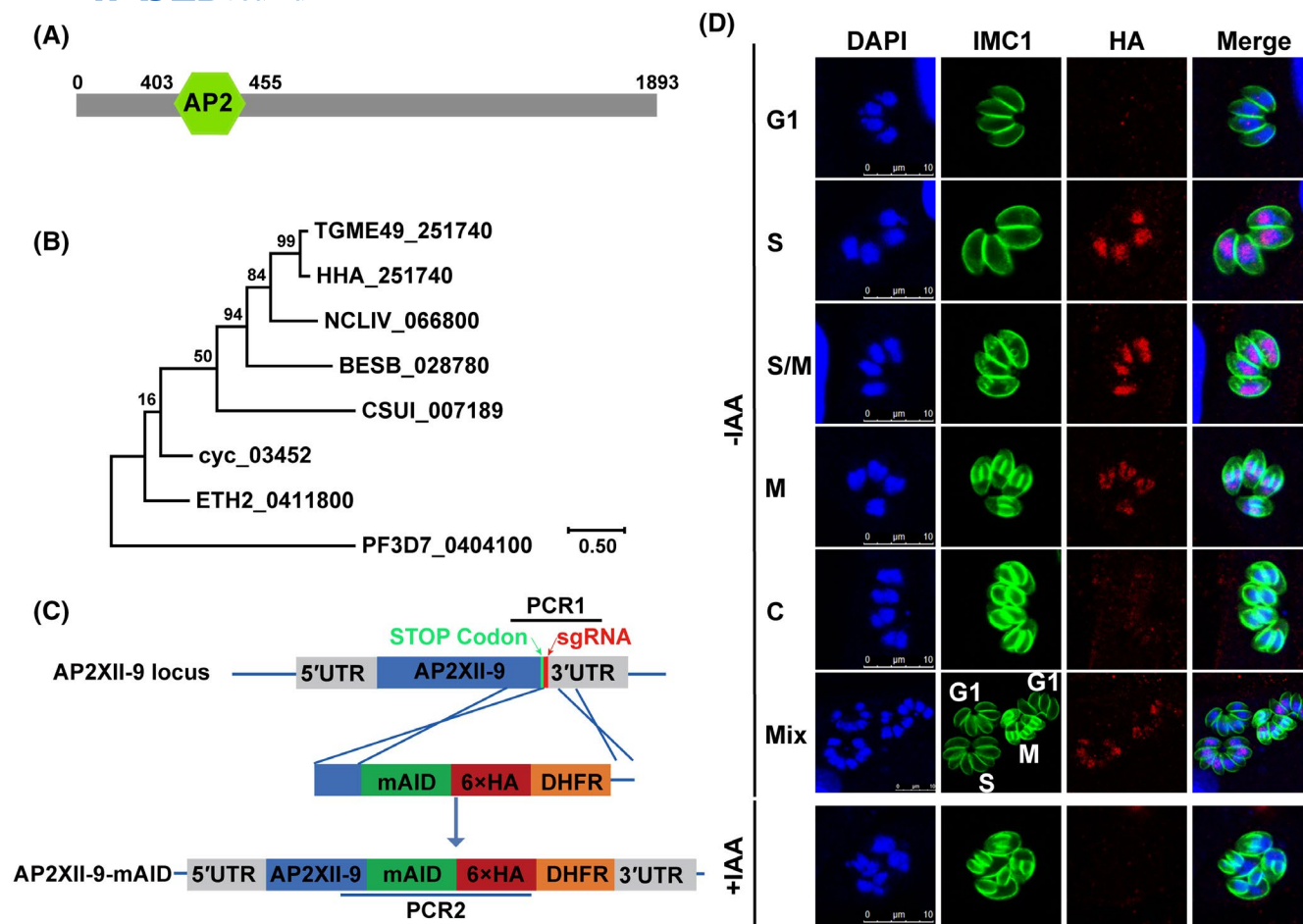
FIGURE 1 Characterization of AP2XII-9 and generation of AP2XII-9-mAID strain in *T. gondii*. (A) Domain analysis of AP2XII-9 using ExPASy Server (https://www.expasy.org) showed that the AP2 domain (amino acids 403–455) is located in the N-terminal ⅓ of AP2XII-9 protein. (B) Basic biological information on all apicomplexan parasites was obtained from VEuPathDB (https://veupathdb.org/veupathdb/app/). Homologous proteins were screened using Blast function of VEuPathDB. The maximum likelihood method and a JTT matrix-based model were used to construct the phylogenetic tree of AP2XII-9. Evolutionary analysis using MEGA X showed that AP2XII-9 is widely conserved across apicomplexan parasites. (C) Schematic representation of generation of AP2XII-9-mAID lines in *T. gondii* using mAID system and CRISPR-Cas9 method. (D) IFA results showed that AP2XII-9 is dynamically expressed in the nucleus, with peak expression during the S/M phase and low or undetectable expression in the G1 and C phases. AP2XII-9 protein was degraded in the AP2XII-9-mAID strain treated with IAA for 24 h. Tachyzoites were cultured for 24 h, and the parasite's localization and nucleus were labeled using rabbit anti-IMC1 (green), mouse anti-HA (red), and DAPI (blue). Scale bar = 10 μm.

in HFFs with or without IAA for 24 h. The degradation of AP2XII-9 under IAA treatment had significantly reduced the replication ability (Figure 2E). Finally, for the egress assay, AP2XII-9-mAID tachyzoites were cultured in the presence and absence of IAA for 60 h or 36 h, and egress efficiency was assessed by inducing with 3 μM calcium ionophore A23187. The deletion of AP2XII-9 resulted in significantly decreased ability of induced tachyzoites to egress (Figure 2F). These results demonstrate that AP2XII-9 influences *T. gondii* growth by participating in key processes of the lytic cycle, primarily through its role in replication, further highlighting the importance of AP2XII-9 in the parasite's growth.

3.3 | AP2XII-9 is essential for membrane integrity, normal rosette structure, and synchronous division in type I RH strain

To further investigate the important role of AP2XII-9 in *T. gondii* replication, the RH::TIR1-AP2XII-9-mAID strain was allowed to culture in HFFs for 28 h with or without IAA to visualize parasites using IFA. Results showed that the deletion of AP2XII-9 led to structural and morphological defects in *T. gondii*, manifested as a disorganized rosette structure (i, 84.41 ± 1.71%), damaged IMC1 formation (ii, 34.05 ± 5.93%) as shown by IMC1 staining. Interestingly, asynchronous
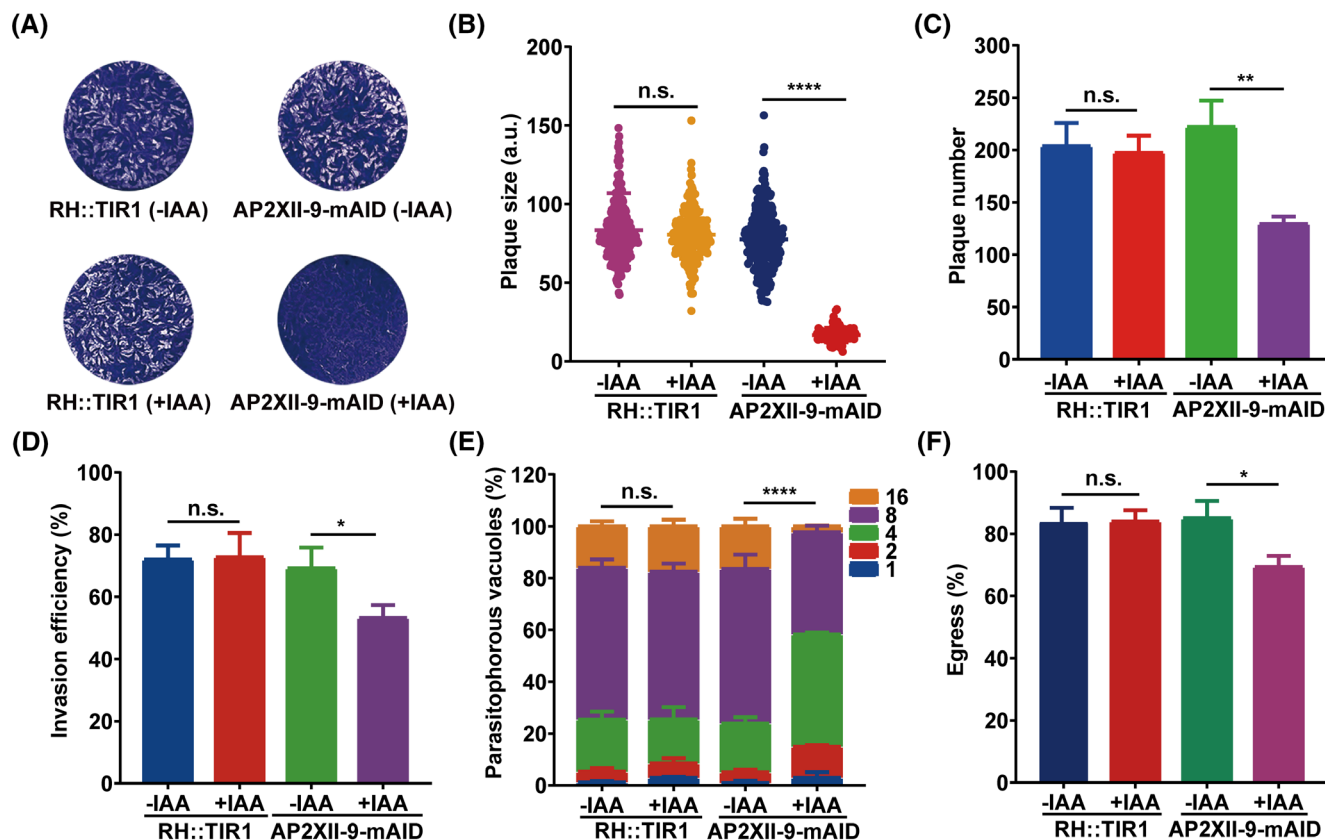
FIGURE 2 AP2XII-9 is essential for the growth of *T. gondii* in type I RH strain. (A) Representative images of plaques of RH::TIR1-AP2XII-9-mAID strain cultured for 7 days with or without IAA under normal culture conditions. (B, C) Quantification of area (B) and number (C) of plaque formation of indicated strains grown in HFFs with or without IAA for 7 days. (D) Quantification of invasion ratio of intracellular tachyzoites and all tachyzoites by pretreating indicated strains with or without IAA for 24 h and invading for 30 min. (E) Quantification of replication ability of indicated strains by culturing for 24 h in the presence or absence of IAA after 1 h invasion. (F) Quantification of egress ability in the presence of the 3 μM calcium ionophore A23187 by treating indicated strains for 60 h or 36 h with or without IAA. The mean ± SD of data of three repeated experiments was calculated. Significance analysis of replication assay was carried out with two-way ANOVA with Tukey multiple comparison test. Plaque formation assay, invasion assay, and egress assay were analyzed by two-tailed, unpaired *t*-test. $*p < .05$, $**p < .01$, $***p < .001$, n.s., not significant.

division (iii, $16.93 \pm 1.51\%$) was also observed in the AP2XII-9-mAID strain treated with IAA (Figure 3A,B).

The integrity of the inner membrane complex, including alveoli, subpellicular network, and motor complex, is essential to maintain the normal morphology and structure of *T. gondii* for efficient infection.[48] Given defects in IMC1, ISP1 affiliated with IMC subcompartment proteins and motor complex components GAP45 were stained to further investigate the defects of membrane formation. IFA results revealed that ISP1, an early progenitor IMC subcompartment protein localized to the apical cap of parasites,[45] was not seldomly altered by the disruption of AP2XII-9 (Figure 3C). However, the AP2XII-9-mAID strain stained with GAP45, which was exclusively expressed in the maternal parasite at the pellicle, between the plasma membrane (PM) and IMC,[49] showed membrane defects similar to those of IMC1 staining under IAA treatment (Figure 3D,E). Interestingly, GAP45 was mostly defective at the site of IMC1 formation defects.

These results indicate that the depletion of AP2XII-9 results in disruption of membrane integrity, rosette structure, and synchronous division.

3.4 | Depletion of AP2XII-9 results in apicoplast defects in type I RH strain

Regular replication, division, and proper assembly of organelles in parasites are the basis of normal growth.[9] To determine the effects of the deletion of AP2XII-9 on other organelles, AP2XII-9-mAID tachyzoites treated with IAA were allowed to stain key organelle markers. Compared with the control group, there were no significant changes in micronemes, dense granules, rhoptries, endoplasmic reticulum, and mitochondria, as shown by the staining of respective organelle markers (MIC2, GRA5, ARO, SERCA, HSP60) (Figure S3A–E). However, up to $21.81 \pm 6.10\%$
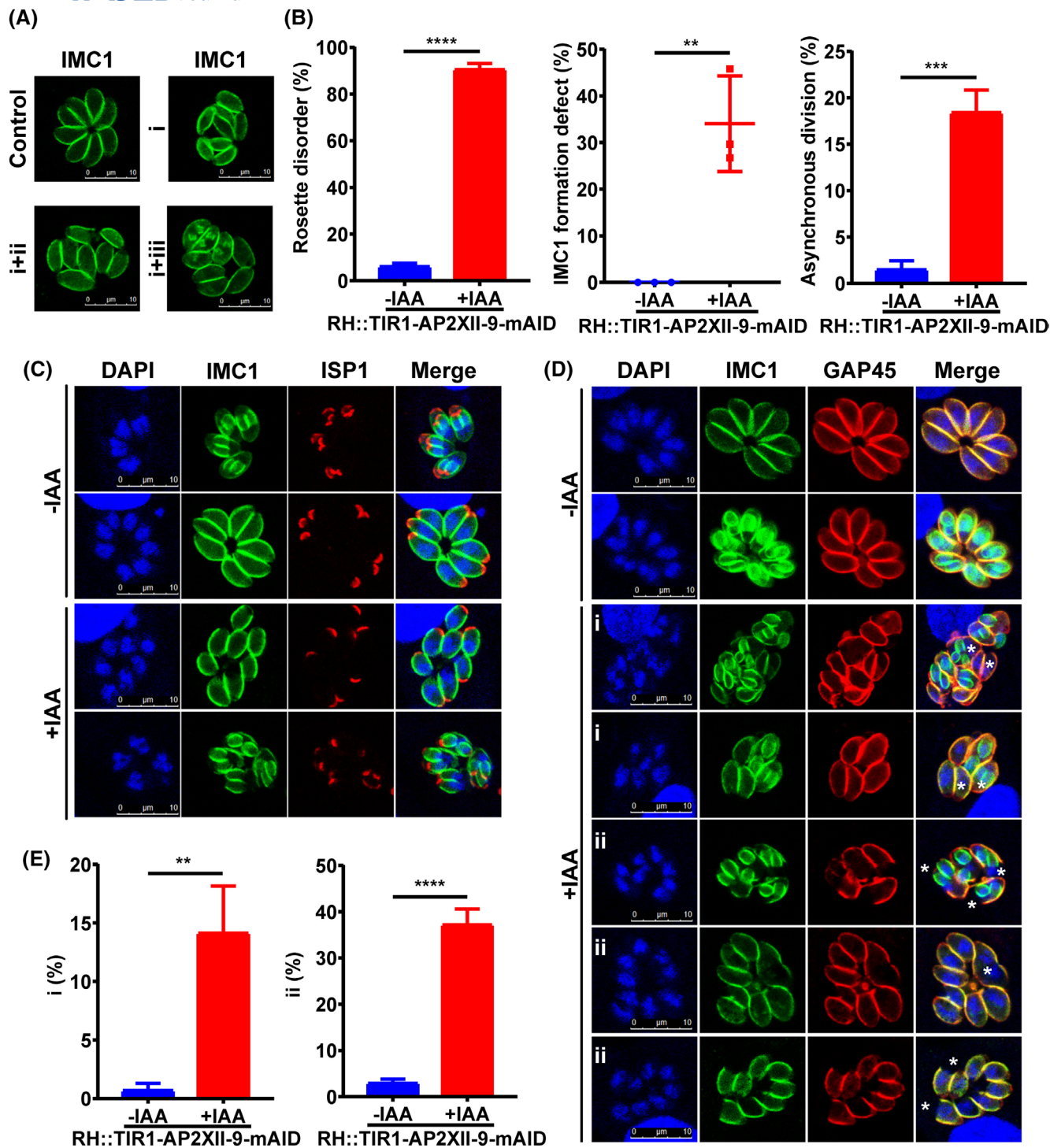
FIGURE 3 AP2XII-9 is important for the maintenance of parasite morphology, structure, and normal division in type I RH strain. (A) IFA results showed that depletion of AP2XII-9 resulted in the destruction of rosette-structure (i), IMC1 integrity (ii), and synchronous division (iii) as shown by IMC label (green). Scale bar = 10 μm. (B) Quantification of defects in IMC1 staining in RH::TIR1-AP2XII-9-mAID strain with or without IAA for 28 h. (C) The structure of ISP1 (red) were unaffected in AP2XII-9-mAID strain with or without IAA for 28 h. (D) RH::TIR1-AP2XII-9-mAID strain stained with GAP45 (red) under IAA treatment showed similar defects as IMC1 staining. Asterisks indicated the places of defects. (i) and (ii) denoted asynchronous division and membrane defect, respectively. Scale bar = 10 μm. (E) Quantification of defects in GAP45 staining in RH::TIR1-AP2XII-9-mAID strain with or without IAA for 28 h. The data in the figures were obtained from mean ± SD of three independent experiments and analyzed for statistical differences by two-tailed, unpaired t-test. **$p < .01$, ***$p < .001$, ****$p < .0001$.
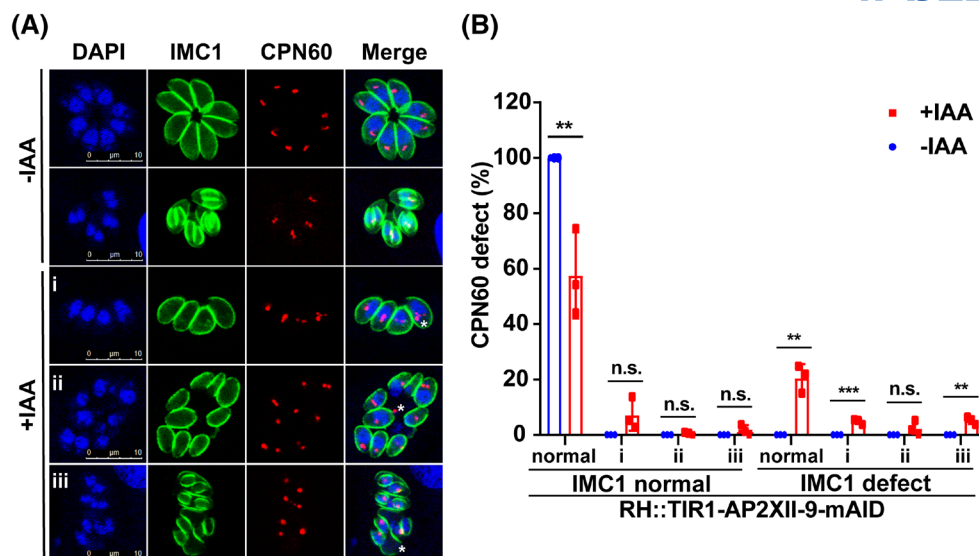
FIGURE 4 AP2XII-9 is important for the correct inheritance of apicoplast in type I RH strain. (A) IFA showed that deletion of AP2XII-9 triggered dysregulated apicoplast inheritance, as indicated by (i) Over-replication apicoplast, (ii) Ectopic apicoplast, and (iii) Absent apicoplast. Scale bar = 10 μm. (B) Quantification of the inheritance dysregulation of apicoplast caused by AP2XII-9 deletion for 28 h. Mean ± SD of three independent repeated experiments was used for data in the figure, and statistical difference analysis was conducted by two-tailed, unpaired t-test. $**p < .01$, $***p < .001$, n.s., not significant.

of RH::TIR1-AP2XII-9-mAID tachyzoites treated with IAA for 28 h produced apicoplast defects, including over-replication (i), ectopic localization (ii), and loss (iii) as indicated by CPN60 (Figure 4A,B). Interestingly, inheritance of the apicoplast is independent of IMC1 defects (Figure 4B). These results suggest that AP2XII-9 contributes to the correct inheritance of the apicoplast.

3.5 | Depletion of AP2XII-9 in cyst-forming type II Pru strain led to more severe asynchronous division defects than in type I RH strain

To confirm the function of AP2XII-9, a mAID system combined with CRISPR-Cas9 technology was similarly implemented in a cyst-forming strain to conditionally regulate the expression of AP2XII-9. Phenotypic analysis (plaque formation, invasion, replication, and egress) showed that depletion of AP2XII-9 caused more pronounced growth defects in the cyst-forming Pru strain, as shown by the inability to form a visible plaque and significantly reduced replication capacity (Figure S4A–F). The depletion of AP2XII-9 in the cyst-forming strain resulted in a similar degree of membrane formation and apicoplast defects, but more severe asynchronized division with the increase of time (28 h IAA: 40.71 ± 2.083%; 36 h IAA: 52.71 ± 1.015%) (Figure 5A–D). These results further confirm the critical role of AP2XII-9 in the growth of *T. gondii*.

3.6 | AP2XII-9 is involved in the process of bradyzoite differentiation

Given that several AP2 factors, such as AP2XII-2, AP2IX-9, and AP2IV-3, are involved in cyst differentiation as either activators or repressors,[19,24,27,44] the role of AP2XII-9 in bradyzoite differentiation was studied. An in vitro bradyzoite differentiation assay was conducted to examine the differentiation of the AP2XII-9-mAID strain under normal conditions, with or without IAA, for 60 h. Interestingly, IFA results showed that the AP2XII-9-mAID strain under IAA treatment significantly increased bradyzoite differentiation compared with those without IAA treatment, manifested by a significantly increased DBL staining (Figure 6A,B). This phenotype was further verified by a significant increase in the expression of bradyzoite-specific antigen BAG1, a canonical marker of late bradyzoite development,[50] as shown by IFA and western blotting (Figure 6A,C), suggesting that AP2XII-9 is important for bradyzoite formation and may function as a repressor.

3.7 | Depletion of AP2XII-9 alters transcriptomic changes of numerous genes related to tachyzoite growth and bradyzoite differentiation

To gain insight into the transcriptomic changes triggered by AP2XII-9 depletion, RNA sequencing was performed
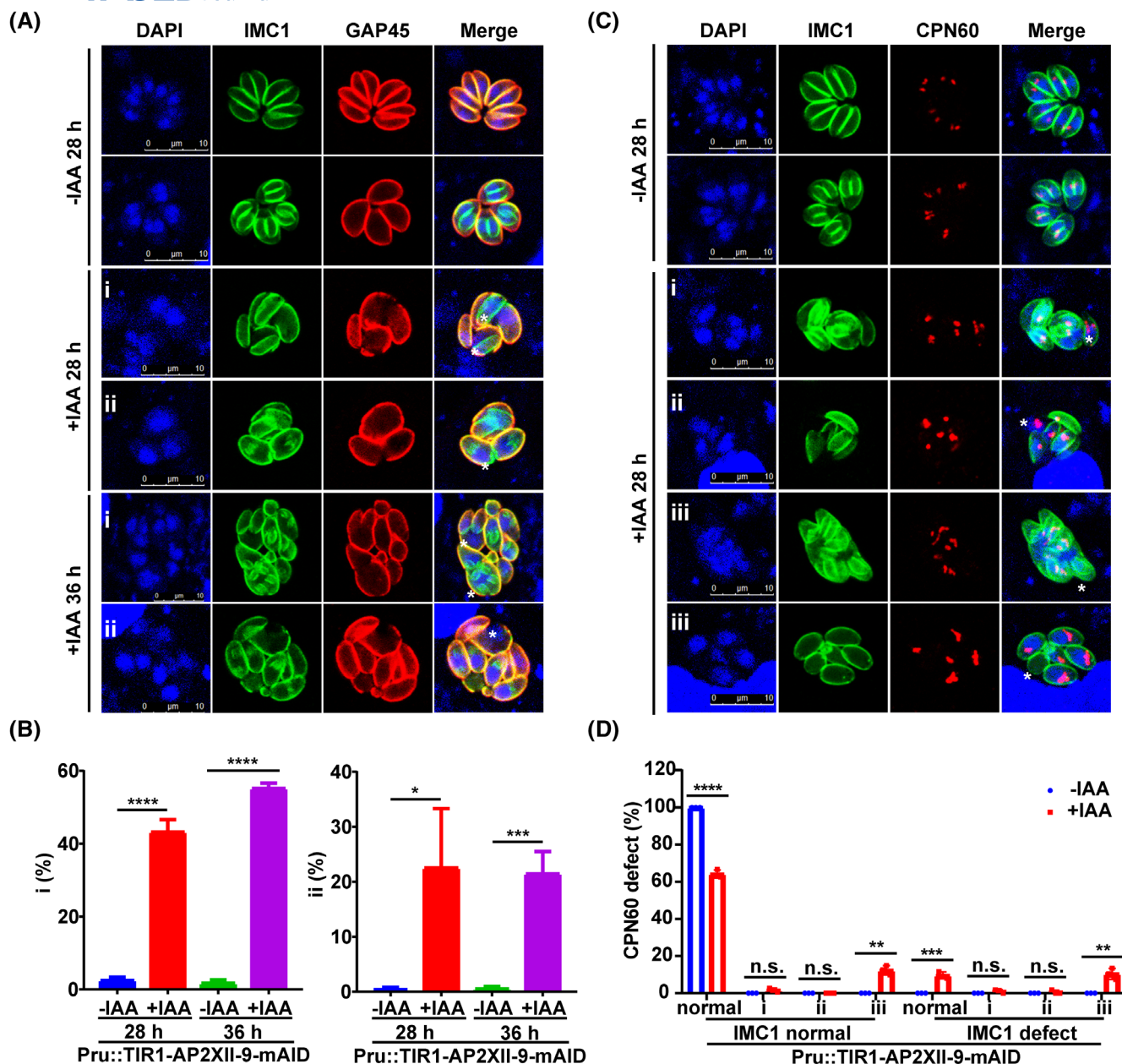
FIGURE 5 Depletion of AP2XII-9 in type II cyst-forming Pru strain resulted in more severe asynchronous division. (A) IFA results showed that with the increase of IAA treatment time, Pru::TIR1-AP2XII-9-mAID strain had higher degree of asynchronous division and similar membrane defects. (i) Asynchronous division, (ii) Defect of membrane formation. White asterisk: The places of defects. Scale bar = 10 μm. (B) Quantification of asynchronous division and membrane defect triggered by treatment of Pru::TIR1-AP2XII-9-mAID strain with IAA for 28 h and 36 h. (C) IFA results revealed that the deletion of AP2XII-9 resulted in dysregulated apicoplast inheritance, as shown by (i) Over-replication apicoplast, (ii) Ectopic apicoplast, and (iii) Absent apicoplast. (D) Quantification of apicoplast dysregulation caused by depletion of AP2XII-9. The mean ± SD of data of three repeated experiments was calculated, and significance analysis was carried out with two-tailed, unpaired t-test. $*p < .05$, $**p < .01$, $***p < .001$, $****p < .0001$, n. s., not significant.

on the Pru::TIR1-AP2XII-9-mAID strain under normal culture conditions with or without IAA for 72 h. The differentially expressed genes (DEGs) were identified by using $|\log_2$ Fold Change$| \geq 1$ and Q values <0.05 as the threshold. A total of 1014 DEGs were identified in the AP2XII-9-mAID strain in the presence or absence of IAA, of which 899 were up-regulated and 115 were down-regulated after

depletion of AP2XII-9. As expected, many genes involved in the important lytic cycle of *T. gondii*, such as MIC1, MIC9, MIC10, MIC11, MIC12, ROP11, ROP24, ROP34, and ROP40, were significantly down-regulated in the Pru::TIR1-AP2XII-9-mAID strain in the presence of IAA compared to the non-IAA-treated group (Figure 7A,B). Interestingly, depletion of AP2XII-9 down-regulated
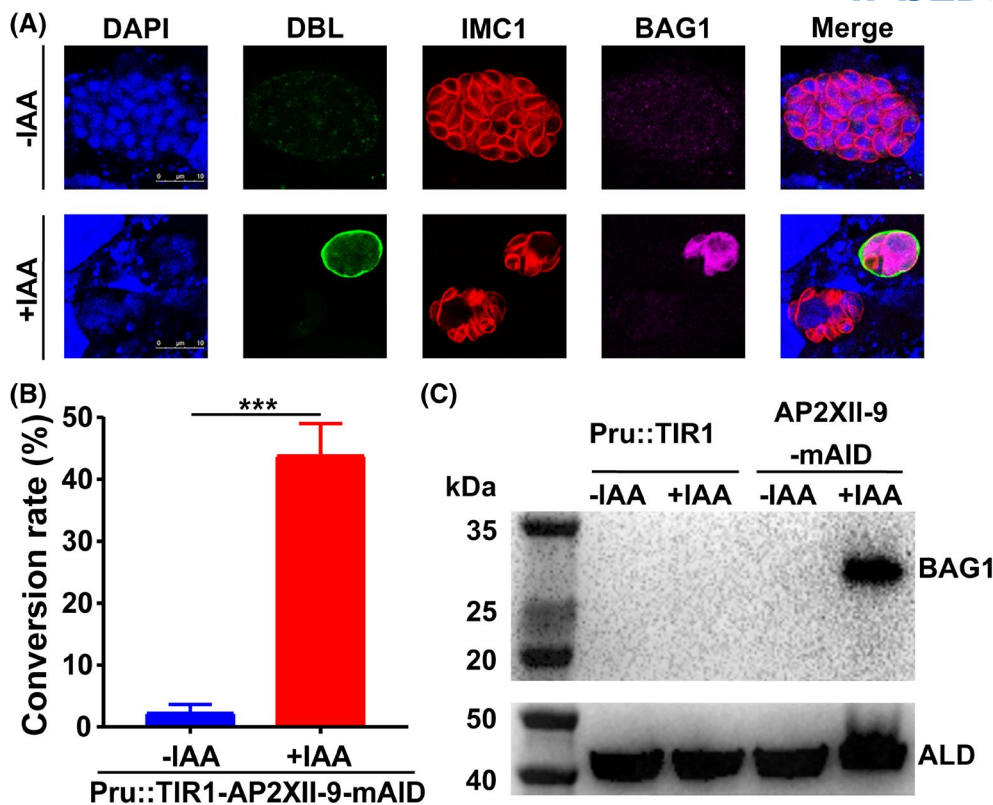
FIGURE 6 Deletion of AP2XII-9 in type II cyst-forming Pru strain increases tachyzoites to bradyzoites differentiation in vitro. (A) Pru::TIR1-AP2XII-9-mAID strain infected HFFs for 60 h under normal culture conditions was stained with rabbit anti-BAG1 (magenta), mouse anti-IMC1 (red), and DBL (green). Scale bar = 10 μm. (B) Quantification of bradyzoite conversion rate of Pru::TIR1-AP2XII-9-mAID strain with or without IAA for 60 h under normal culture conditions. Mean ± SD of three independent repeated experiments was used for data in the figure, and statistical difference analysis was conducted by two-tailed, unpaired t-test. ***$p < .001$. (C) Western blotting confirmed the increased expression of BAG1. Anti-aldolase (ALD) was used as a control.

the expression of genes related to membrane formation and division, such as IMC4, IMC6, IMC10,[51] IMC11,[52] IMC14,[52,53] and SPM1.[54] In addition, apicoplast defects caused by the depletion of AP2XII-9 were further confirmed by the up-regulation of methionine aminopeptidase 2 (MAP2) and MAP1c (Figure 7A,B).[55] These results confirmed that AP2XII-9 plays an important role in the growth of *T. gondii*.

In addition, RNA sequencing showed that some characteristic bradyzoite-specific proteins, including BAG1,[50] LDH2,[56] enolase 1,[57,58] DnaK-TPR,[59] BRP1,[60] AP2IV-3,[24] and MAG1,[61] were significantly up-regulated in AP2XII-9-depleted tachyzoites as shown by DBL and BAG1 staining (Figures 6 and 7C,D). On the contrary, genes that are highly expressed in tachyzoites, such as MIC2, were down-regulated (Figure 7C,D). Eight DEGs, including lytic cycle or bradyzoite differentiation-related genes, were randomly selected, and their expression changes were confirmed by RT-qPCR (Figure 7E and Table S1). These results further suggest that AP2XII-9 may act as a repressor by affecting bradyzoite-associated proteins involved in cyst differentiation.

4 | DISCUSSION

The flexible transformation from rapid replicating tachyzoites to slow-growing bradyzoites of *T. gondii* is closely related to the establishment of chronic infection and the maintenance of long-term infection.[62] Several transcription factors, including members of the AP2 family, are involved in stage transformation as either activators or repressors.[19,24,28] However, the functions of many other transcription factors within the AP2 family remain unclear. In this study, we investigated the AP2 transcription factor AP2XII-9 and found that it is periodically expressed during the tachyzoite stage and is essential for parasite growth by influencing normal cell division, as well as the assembly of organelles and the inner membrane complex. Additionally, AP2XII-9 actively regulates bradyzoite differentiation by inhibiting the expression of bradyzoite-specific genes, indicating that AP2XII-9 plays crucial roles in ensuring proper cell cycle progression and may function as a repressor regulating bradyzoite differentiation.

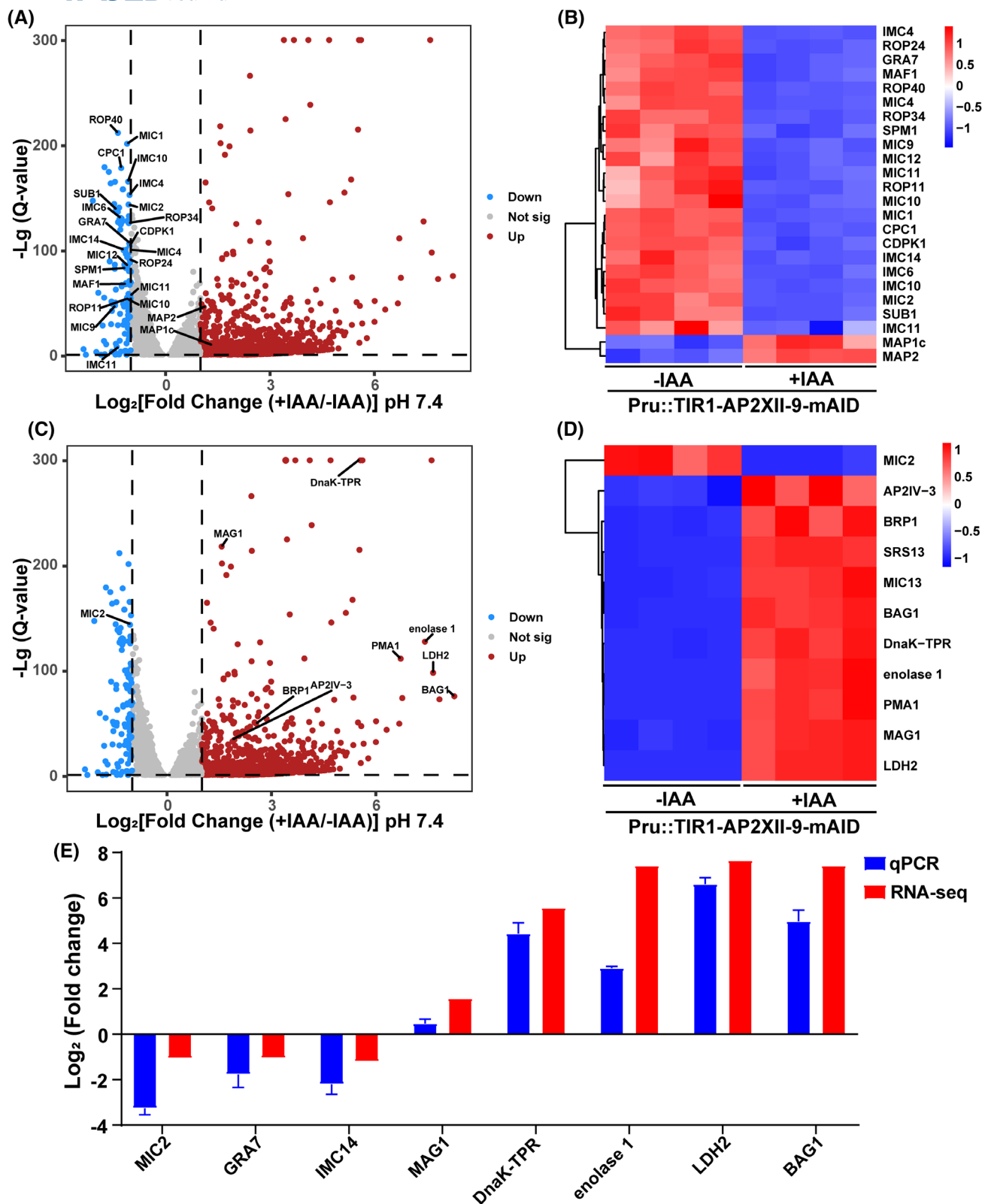Several AP2 factors in tachyzoites exhibit specific expression profiles that are indicative of cell cycle stage.[21]

FIGURE 7 Transcriptomic analysis of Pru::TIR1-AP2XII-9-mAID strain in the presence or absence of IAA for 72 h under normal culture conditions. (A–D) Volcano plot (A, C) and heat map (B, D) illustrated decreased expression of growth associated proteins (A, B) and increased expression of characteristic bradyzoites specific proteins (C, D) in the AP2XII-9-depeletd parasites. Genes with up-regulated, down-regulated, and no significant changes in the volcano plots were marked in red, blue, and gray, respectively. Four replicates were set up for each set of samples. (E) Real-time quantitative PCR (RT-qPCR) confirmed the expression of eight randomly selected genes related to lytic cycle or bradyzoite differentiation in the presence or absence of AP2XII-9.

As an AP2 transcription factor, AP2XII-9 was expressed exclusively in the nucleus and showed periodic expression during the tachyzoite stage. Its expression was detected in the S phase, peaked in the late S and early M phases, decreased in the late M phase, and was low or undetectable in the G1 and C phases. Among the identified AP2 factors, some factors, such as AP2IX-4, AP2IV-4, and AP2XII-2, exhibited a similar expression trend to AP2XII-9, but these factors have the similar or different roles in growth and stage differentiation. For example, AP2IX-4 and AP2IV-4 are dispensable for parasite growth, while AP2XII-2 is essential.[20,26,44] Surprisingly, AP2IX-4, AP2IV-4, and AP2XII-2 act as repressors in bradyzoite transformation, but how these three genes work together to inhibit stage differentiation and what role AP2XII-9 plays in bradyzoite development under similar expression patterns remain unclear.[20,26,44] Therefore, it is urgent to investigate the role of AP2XII-9 in the growth and stage transformation of *T. gondii*.

To elucidate the biological function of AP2XII-9, conditional knockout strains of type I RH strain and type II Pru strain were generated using the mAID system and CRISPR-Cas9 technology. As expected, phenotypic experiments suggested that AP2XII-9 is essential for the growth of *T. gondii*. The tachyzoite of *T. gondii* divides into two daughter parasites by endodyogeny, which involves the emergence and assembly of the daughter parasites, the dissociation of the mother parasites, and the synthesis and packaging of the related organelles.[9] Depletion of AP2XII-9 resulted in significantly increased asynchronous division and membrane defects. Transcriptomic analysis showed that deletion of AP2XII-9 caused downregulation of several related factors, such as IMC4 and SPM1, which are associated with maintaining the stability of the inner membrane complex,[54,63] while IMC10 and IMC14 are considered to be involved in the switch between endodyogeny and endopolygeny.[51,52] The integrity of IMC provides the mechanical strength for parasite survival in different environments and enhances parasite fitness.[48,64,65] The IMC serves as the anchor of the actin-myosin motor complex (atypical myosin MyoA-MLC1-ELC1 and glideosome-associated proteins GAP40, GAP45, and GAP50), which plays important roles in parasite movement and invasion.[66] Membrane defects demonstrated by IMC1 and GAP45 staining appear to provide a reason for the impaired infectivity caused by the depletion of AP2XII-9. However, given the similar locations of membrane defects stained by IMC1 and GAP45, future studies need to explore the mechanism of how AP2XII-9 mediates IMC1 and GAP45 to regulate membrane formation.

On the other hand, depletion of AP2XII-9 did not affect the structure of micronemes, dense granules, rhoptries, endoplasmic reticulum, and mitochondria. However,

it did cause inheritance defects in the apicoplast, manifested by apicoplast over-replication, loss, and ectopic localization. Transcriptomic analysis revealed that deletion of AP2XII-9 led to increased expression of MAP2 and MAP1c, which are involved in apicoplast biosynthesis.[55] Multiple metabolic pathways regulated by the apicoplast, including heme, fatty acid, lysophosphatidic acid, and isopentenyl pyrophosphate synthesis pathways, are closely related to the maintenance and expansion of the infection in *T. gondii*, ensuring optimal fitness in vitro.[67–69] Depletion of AP2XII-9 may lead to a disturbance of the metabolic pathways regulated by the apicoplast, impairing the optimal fitness of *T. gondii*. These results suggest that AP2XII-9 is important for *T. gondii* growth through the maintenance of normal morphology, structure, and tachyzoite cell cycle division.

Interestingly, while preparing this manuscript, two independent research groups also demonstrated that AP2XII-9 affects parasite asexual division and disrupts apicoplast inheritance by regulating the expression of key genes involved in the parasite's lytic cycle using RNA sequencing and targeting genes related to the moving junction and inner membrane complex through Cleavage Under Targets and Tagmentation (CUT&Tag).[70,71] These two studies draw some conclusions similar to those presented in our article, confirming the role of AP2XII-9 in the growth of the type I RH strain of *T. gondii*. However, neither of these two published studies has investigated the involvement of AP2XII-9 in the conversion from tachyzoites to bradyzoites. Given that the cell cycle of tachyzoites is closely related to bradyzoite differentiation, in which several AP2 factors are involved,[72] the role of AP2XII-9 in bradyzoite differentiation was further investigated in our study.

Tachyzoites to bradyzoites differentiation occurs in the S/M phase, and its formation requires slower tachyzoite growth, which is manifested by slower protein synthesis in the G1 phase to prolong the G1 phase and delay the S phase.[72,73] As expected, deletion of AP2XII-9 led to a significant increase in bradyzoite transformation, as shown by DBL and BAG1 staining. AP2XII-9 fits some typical characteristics of AP2 factors involved in stage transformation, such as peak expression of AP2XII-9 in the S/M phase, and depletion of AP2XII-9 caused slower parasite growth. Transcriptomic analysis revealed that AP2XII-9 regulated bradyzoite formation by down-regulating several bradyzoite-specific genes (MAG1,[61] LDH2,[56] enolase 1,[57] DnaK-TPR,[59] BAG1,[50] BRP1,[60] AP2IX-9,[19,24] AP2IV-3,[24] AP2Ib-1,[24,74] and AP2VIIa-1[20,24]) and up-regulating a tachyzoite-specific gene MIC2.[75] AP2Ib-1, AP2VIIa-1, AP2IX-9, and AP2IV-3, which are expressed in the early stage of bradyzoites under stress induction,[24] were up-regulated in the absence of AP2XII-9, indicating that

they may play important roles in coordinating bradyzoite transformation. Notably, AP2IX-9 and AP2IV-3 exhibit opposing roles in the regulation of bradyzoite development. AP2IX-9 acts as a repressor, inhibiting bradyzoite formation, while AP2IV-3 functions as an activator, promoting bradyzoite development.[19,24] In addition, AP2XII-9 shares a similar expression pattern with AP2IX-4, AP2IV-4, and AP2XII-2, which also play similar roles in inhibiting bradyzoite development, as indicated by the up-regulated expression of bradyzoite development-related factors after the depletion or disruption of these genes.[20,26,44] These findings underscore the importance of the coordinated expression of multiple AP2 factors in ensuring the timely transition to the bradyzoite stage, highlighting the complexity of the bradyzoite development pathway.

Studies have further classified transcriptional repressors into active and passive repressors.[76] Like AP2IV-4,[20] deletion of AP2XII-9 actively leads to dysregulation of bradyzoite-specific protein expression without external stimulation. In contrast, AP2IX-9,[19,24] AP2XII-2,[44] and AP2IX-4[26] are passive repressors of bradyzoite transformation, suppressing the expression of bradyzoite-specific genes at the tachyzoite stage. These results suggest that these AP2 factors act as active or passive repressors of cyst formation to collectively prevent the process of bradyzoite development and ensure normal progression of life cycle stages, but how the regulatory networks formed by AP2XII-9 interact with other AP2 factors to jointly influence bradyzoite progression remains the focus of future research.

In conclusion, depletion of AP2XII-9 impairs parasite growth by affecting important lytic processes, leading to defects in membrane structure, apicoplast assembly, and synchronous division. In addtion, depletion of AP2XII-9 increases the bradyzoite differentiation, suggesting that AP2XII-9 may function as an active repressor, regulating bradyzoite differentiation by controlling the expression of bradyzoite specific proteins. Our study reinforces the link between tachyzoite cell cycle progression and bradyzoite differentiation, while expanding the understanding of AP2 factors in parasite division, assembly of organelles, as well as inner membrane complex.

AUTHOR CONTRIBUTIONS

Jin-Lei Wang, Xing-Quan Zhu and Meng Wang conceived and designed the experiments. Xiao-Jing Wu, Meng Wang and Jin Gao performed the experiments, analyzed the data and wrote the article. Nian-Zhang Zhang, Ting-Ting Li and Li-Xiu Sun participated in the implementation of the study. Jin-Lei Wang, Xing-Quan Zhu, Meng Wang and Nian-Zhang Zhang critically revised the manuscript. Jin-Lei Wang, Meng Wang and Xing-Quan Zhu secured funds and supervised the project. All authors read and approved the final version of the manuscript.

DISCLOSURES

The authors declare that they have no competing interests.

DATA AVAILABILITY STATEMENT

The RNA sequencing raw data that support the findings of this study are available in the NCBI Short Read Archive database (https://www.ncbi.nlm.nih.gov/sra) under the bioproject number PRJNA1173514.

ORCID

Xiao-Jing Wu https://orcid.org/0009-0008-3724-0776
Meng Wang https://orcid.org/0009-0008-1738-9653
Nian-Zhang Zhang https://orcid.org/0009-0007-2148-2060
Ting-Ting Li https://orcid.org/0000-0002-8485-4630
Jin Gao https://orcid.org/0009-0002-8511-5917
Li-Xiu Sun https://orcid.org/0009-0003-0894-847X
Xing-Quan Zhu https://orcid.org/0000-0003-2530-4628
Jin-Lei Wang https://orcid.org/0000-0002-2373-9049

REFERENCES

1. Wang ZD, Wang SC, Liu HH, et al. Prevalence and burden of *Toxoplasma gondii* infection in HIV-infected people: a systematic review and meta-analysis. *Lancet HIV*. 2017;4:e177-e188.
2. Galal L, Ariey F, Gouilh MA, et al. A unique *Toxoplasma gondii* haplotype accompanied the global expansion of cats. *Nat Commun*. 2022;13:5778.
3. Sokol SL, Primack AS, Nair SC, et al. Dissection of the *in vitro* developmental program of *Hammondia hammondi* reveals a link between stress sensitivity and life cycle flexibility in *Toxoplasma gondii*. *elife*. 2018;7:e36491. doi:10.7554/eLife.36491
4. Montoya JG, Liesenfeld O. Toxoplasmosis. *Lancet*. 2004;363:1965-1976.
5. Elsheikha HM, Marra CM, Zhu XQ. Epidemiology, pathophysiology, diagnosis, and management of cerebral toxoplasmosis. *Clin Microbiol Rev*. 2021;34:e00115-e00119.
6. Dubey JP, Lindsay DS, Speer CA. Structures of *Toxoplasma gondii* tachyzoites, bradyzoites, and sporozoites and biology and development of tissue cysts. *Clin Microbiol Rev*. 1998;11:267-299.
7. Francia ME, Striepen B. Cell division in apicomplexan parasites. *Nat Rev Microbiol*. 2014;12:125-136.

8. Blader IJ, Coleman BI, Chen CT, Gubbels MJ. Lytic cycle of *Toxoplasma gondii*: 15 years later. *Ann Rev Microbiol*. 2015;69:463-485.

9. Verhoef JMJ, Meissner M, Kooij TWA. Organelle dynamics in apicomplexan parasites. *MBio*. 2021;12:e0140921.

10. Ouologuem DT, Roos DS. Dynamics of the *Toxoplasma gondii* inner membrane complex. *J Cell Sci*. 2014;127:3320-3330.

11. Radke JR, Striepen B, Guerini MN, Jerome ME, Roos DS, White MW. Defining the cell cycle for the tachyzoite stage of *Toxoplasma gondii*. *Mol Biochem Parasitol*. 2001;115:165-175.

12. Marq JB, Gosetto M, Altenried A, et al. Cytokinetic abscission in *Toxoplasma gondii* is governed by protein phosphatase 2A and the daughter cell scaffold complex. *EMBO J*. 2024;43:3752-3786.

13. Khelifa AS, Guillen Sanchez C, Lesage KM, et al. TgAP2IX-5 is a key transcriptional regulator of the asexual cell cycle division in *Toxoplasma gondii*. *Nat Commun*. 2021;12:116.

14. Li Y, Niu Z, Yang J, et al. Rapid metabolic reprogramming mediated by the AMP-activated protein kinase during the lytic cycle of *Toxoplasma gondii*. *Nat Commun*. 2023;14:422.

15. Licon MH, Giuliano CJ, Chan AW, et al. A positive feedback loop controls *Toxoplasma* chronic differentiation. *Nat Microbiol*. 2023;8(5):889-904. doi:10.1038/s41564-023-01358-2

16. Waldman BS, Schwarz D, Wadsworth MH 2nd, Saeij JP, Shalek AK, Lourido S. Identification of a master regulator of differentiation in *Toxoplasma*. *Cell*. 2020;180:359-372.e316.

17. Wang JL, Li TT, Elsheikha HM, et al. The protein phosphatase 2A holoenzyme is a key regulator of starch metabolism and bradyzoite differentiation in *Toxoplasma gondii*. *Nat Commun*. 2022;13:7560.

18. Wang JL, Li TT, Zhang NZ, et al. The transcription factor AP2XI-2 is a key negative regulator of *Toxoplasma gondii* merogony. *Nat Commun*. 2024;15:793.

19. Radke JB, Lucas O, De Silva EK, et al. ApiAP2 transcription factor restricts development of the *Toxoplasma* tissue cyst. *Proc Natl Acad Sci USA*. 2013;110:6871-6876.

20. Radke JB, Worth D, Hong D, et al. Transcriptional repression by ApiAP2 factors is central to chronic toxoplasmosis. *PLoS Pathog*. 2018;14:e1007035.

21. Behnke MS, Wootton JC, Lehmann MM, et al. Coordinated progression through two subtranscriptomes underlies the tachyzoite cycle of *Toxoplasma gondii*. *PLoS One*. 2010;5:e12354.

22. Zarringhalam K, Ye S, Lou J, Rezvani Y, Gubbels MJ. Cell cycle-regulated ApiAP2s and parasite development: the *Toxoplasma* paradigm. *Curr Opin Microbiol*. 2023;76:102383.

23. Feng K, Hou XL, Xing GM, et al. Advances in AP2/ERF superfamily transcription factors in plant. *Crit Rev Biotechnol*. 2020;40:750-776.

24. Hong DP, Radke JB, White MW. Opposing transcriptional mechanisms regulate *Toxoplasma* development. *mSphere*. 2017;2:e00347-e00316.

25. Walker R, Gissot M, Croken MM, et al. The *Toxoplasma* nuclear factor TgAP2XI-4 controls bradyzoite gene expression and cyst formation. *Mol Microbiol*. 2013;87:641-655.

26. Huang S, Holmes MJ, Radke JB, et al. *Toxoplasma gondii* AP2IX-4 regulates gene expression during bradyzoite development. *mSphere*. 2017;2(2):e00054-e00017. doi:10.1128/msphere.00054-17

27. Srivastava S, Holmes MJ, White MW, Sullivan WJ Jr. *Toxoplasma gondii* AP2XII-2 contributes to transcriptional repression for sexual commitment. *mSphere*. 2023;8:e0060622.

28. Zhang J, Fan F, Zhang L, Shen B. Nuclear factor AP2X-4 governs the expression of cell cycle- and life stage-regulated genes and is critical for *Toxoplasma* growth. *Microbiol Spectr*. 2022;10:e0012022.

29. Gao J, Wu XJ, Zheng XN, et al. Functional characterization of eight zinc finger motif-containing proteins in *Toxoplasma gondii* type I RH strain using the CRISPR-Cas9 system. *Pathogens*. 2023;12:1232.

30. Brown KM, Long S, Sibley LD. Conditional knockdown of proteins using auxin-inducible degron (AID) fusions in *Toxoplasma gondii*. *Bio Protoc*. 2018;8:e2728.

31. Li TT, Zhao DY, Liang QL, et al. The antioxidant protein glutaredoxin 1 is essential for oxidative stress response and pathogenicity of *Toxoplasma gondii*. *FASEB J*. 2023;37:e22932.

32. Liang QL, Nie LB, Elsheikha HM, et al. The *Toxoplasma* protein phosphatase 6 catalytic subunit (TgPP6C) is essential for cell cycle progression and virulence. *PLoS Pathog*. 2023;19:e1011831.

33. Wang JL, Bai MJ, Elsheikha HM, et al. Novel roles of dense granule protein 12 (GRA12) in *Toxoplasma gondii* infection. *FASEB J*. 2020;34(2):3165-3178. doi:10.1096/fj.201901416RR

34. Schneider CA, Rasband WS, Eliceiri KW. NIH image to ImageJ: 25 years of image analysis. *Nat Methods*. 2012;9:671-675.

35. Zheng XN, Sun LX, Elsheikha HM, et al. A newly characterized dense granule protein (GRA76) is important for the growth and virulence of *Toxoplasma gondii*. *Int J Parasitol*. 2024;54:109-121.

36. Liu Y, Schmidt B. Long read alignment based on maximal exact match seeds. *Bioinformatics*. 2012;28:i318-i324.

37. Li B, Dewey CN. RSEM: accurate transcript quantification from RNA-Seq data with or without a reference genome. *BMC Bioinformatics*. 2011;12:323.

38. Gajria B, Bahl A, Brestelli J, et al. ToxoDB: an integrated *Toxoplasma gondii* database resource. *Nucleic Acids Res*. 2008;36:D553-D556.

39. Love MI, Huber W, Anders S. Moderated estimation of fold change and dispersion for RNA-seq data with DESeq2. *Genome Biol*. 2014;15:550.

40. Artimo P, Jonnalagedda M, Arnold K, et al. ExPASy: SIB bioinformatics resource portal. *Nucleic Acids Res*. 2012;40:W597-W603.

41. Kumar S, Stecher G, Li M, Knyaz C, Tamura K. MEGA X: molecular evolutionary genetics analysis across computing platforms. *Mol Biol Evol*. 2018;35:1547-1549.

42. Alvarez-Jarreta J, Amos B, Aurrecoechea C, et al. VEuPathDB: the eukaryotic pathogen, vector and host bioinformatics resource center in 2023. *Nucleic Acids Res*. 2024;52:D808-D816.

43. Jones DT, Taylor WR, Thornton JM. The rapid generation of mutation data matrices from protein sequences. *Comput Appl Biosci*. 1992;8:275-282.

44. Srivastava S, White MW, Sullivan WJ Jr. *Toxoplasma gondii* AP2XII-2 contributes to proper progression through S-phase of the cell cycle. *mSphere*. 2020;5:e00542-e00520.

45. Beck JR, Rodriguez-Fernandez IA, de Leon JC, et al. A novel family of *Toxoplasma* IMC proteins displays a hierarchical organization and functions in coordinating parasite division. *PLoS Pathog*. 2010;6(9):e1001094. doi:10.1371/journal.ppat.1001094

46. Morrissette N. Targeting *Toxoplasma* tubules: tubulin, microtubules, and associated proteins in a human pathogen. *Eukaryot Cell*. 2015;14:2-12.

47. Black MW, Boothroyd JC. Lytic cycle of *Toxoplasma gondii*. *Microbiol Mol Biol Rev*. 2000;64:607-623.

48. Harding CR, Meissner M. The inner membrane complex through development of *Toxoplasma gondii* and *Plasmodium*. *Cell Microbiol*. 2014;16:632-641.

49. Gilk SD, Gaskins E, Ward GE, Beckers CJ. GAP45 phosphorylation controls assembly of the *Toxoplasma* myosin XIV complex. *Eukaryot Cell*. 2009;8:190-196.

50. Bohne W, Gross U, Ferguson DJ, Heesemann J. Cloning and characterization of a bradyzoite-specifically expressed gene (hsp30/bag1) of *Toxoplasma gondii*, related to genes encoding small heat-shock proteins of plants. *Mol Microbiol*. 1995;16:1221-1230.

51. Oliveira Souza RO, Jacobs KN, Back PS, Bradley PJ, Arrizabalaga G. IMC10 and LMF1 mediate mitochondrial morphology through mitochondrion-pellicle contact sites in *Toxoplasma gondii*. *J Cell Sci*. 2022;135:jcs260083.

52. Dubey R, Harrison B, Dangoudoubiyam S, et al. Differential roles for inner membrane complex proteins across *Toxoplasma gondii* and *Sarcocystis neurona* development. *mSphere*. 2017;2:e00409-e00417.

53. Cruz-Mirón R, Ramírez-Flores CJ, Lagunas-Cortés N, et al. Proteomic characterization of the pellicle of *Toxoplasma gondii*. *J Proteome*. 2021;237:104146.

54. Tran JQ, Li C, Chyan A, Chung L, Morrissette NS. SPM1 stabilizes subpellicular microtubules in *Toxoplasma gondii*. *Eukaryot Cell*. 2012;11:206-216.

55. Zheng J, Su W, Cao S, Zhang Z, Du C, Jia H. TgMAP1c is involved in apicoplast biogenesis in *Toxoplasma gondii*. *Int J Parasitol*. 2020;50:487-499.

56. Abdelbaset AE, Fox BA, Karram MH, Abd Ellah MR, Bzik DJ, Igarashi M. Lactate dehydrogenase in *Toxoplasma gondii* controls virulence, bradyzoite differentiation, and chronic infection. *PLoS One*. 2017;12:e0173745.

57. Mouveaux T, Oria G, Werkmeister E, et al. Nuclear glycolytic enzyme enolase of *Toxoplasma gondii* functions as a transcriptional regulator. *PLoS One*. 2014;9:e105820.

58. Tomavo S. The differential expression of multiple isoenzyme forms during stage conversion of *Toxoplasma gondii*: an adaptive developmental strategy. *Int J Parasitol*. 2001;31:1023-1031.

59. Yang J, Zhang L, Diao H, et al. ANK1 and DnaK-TPR, two tetratricopeptide repeat-containing proteins primarily expressed in *Toxoplasma* bradyzoites, do not contribute to bradyzoite differentiation. *Front Microbiol*. 2017;8:2210.

60. Schwarz JA, Fouts AE, Cummings CA, Ferguson DJ, Boothroyd JC. A novel rhoptry protein in *Toxoplasma gondii* bradyzoites and merozoites. *Mol Biochem Parasitol*. 2005;144:159-166.

61. Ferguson DJ, Parmley SF. *Toxoplasma gondii* MAG1 protein expression. *Trends Parasitol*. 2002;18:482.

62. Jeffers V, Tampaki Z, Kim K, Sullivan WJ Jr. A latent ability to persist: differentiation in *Toxoplasma gondii*. *Cell Mol Life Sci*. 2018;75:2355-2373.

63. Anderson-White BR, Ivey FD, Cheng K, et al. A family of intermediate filament-like proteins is sequentially assembled into the cytoskeleton of *Toxoplasma gondii*. *Cell Microbiol*. 2011;13:18-31.

64. Mann T, Gaskins E, Beckers C. Proteolytic processing of TgIMC1 during maturation of the membrane skeleton of *Toxoplasma gondii*. *J Biol Chem*. 2002;277:41240-41246.

65. Back PS, Senthilkumar V, Choi CP, et al. The *Toxoplasma* subpellicular network is highly interconnected and defines parasite shape for efficient motility and replication. 2023. bioRxiv.2023.08.10.552545. doi:10.1101/2023.08.10.552545

66. Opitz C, Soldati D. The glideosome: a dynamic complex powering gliding motion and host cell invasion by *Toxoplasma gondii*. *Mol Microbiol*. 2002;45:597-604.

67. Sanchez SG, Bassot E, Cerutti A, et al. The apicoplast is important for the viability and persistence of *Toxoplasma gondii* bradyzoites. *Proc Natl Acad Sci USA*. 2023;120:e2309043120.

68. Seeber F, Soldati-Favre D. Metabolic pathways in the apicoplast of apicomplexa. *Int Rev Cell Mol Biol*. 2010;281:161-228.

69. Kloehn J, Lacour CE, Soldati-Favre D. The metabolic pathways and transporters of the plastid organelle in apicomplexa. *Curr Opin Microbiol*. 2021;63:250-258.

70. Shi Y, Li X, Xue Y, Hu D, Song X. Cell cycle-regulated transcription factor AP2XII-9 is a key activator for asexual division and apicoplast inheritance in *Toxoplasma gondii* tachyzoite. *MBio*. 2024;15:e0133624.

71. Bhaskaran M, Mudiyam V, Mouveaux T, Roger E, Gissot M. Cascading expression of ApiAP2 transcription factors controls daughter cell assembly in *Toxoplasma gondii*. *PLoS Pathog*. 2024;20:e1012810.

72. Radke JR, Guerini MN, Jerome M, White MW. A change in the premitotic period of the cell cycle is associated with bradyzoite differentiation in *Toxoplasma gondii*. *Mol Biochem Parasitol*. 2003;131:119-127.

73. Bohne W, Heesemann J, Gross U. Reduced replication of *Toxoplasma gondii* is necessary for induction of bradyzoite-specific antigens: a possible role for nitric oxide in triggering stage conversion. *Infect Immun*. 1994;62:1761-1767.

74. Xue L, Zhang J, Zhang L, et al. A novel nuclear protein complex controlling the expression of developmentally regulated genes in *Toxoplasma gondii*. *Adv Sci Weinh*. 2025;12:e2412000.

75. Harker KS, Jivan E, McWhorter FY, Liu WF, Lodoen MB. Shear forces enhance *Toxoplasma gondii* tachyzoite motility on vascular endothelium. *MBio*. 2014;5:e01111-e01113.

76. Licausi F, Ohme-Takagi M, Perata P. APETALA2/ethylene responsive factor (AP2/ERF) transcription factors: mediators of stress responses and developmental programs. *New Phytol*. 2013;199:639-649.

SUPPORTING INFORMATION

Additional supporting information can be found online in the Supporting Information section at the end of this article.